EVIDENCE FOR GRAIN GROWTH IN THE PROTOSTELLAR DISKS OF ORION[1]

R. Y. SHUPING

Division of Astronomy and Astrophysics, University of California at Los Angeles,
Los Angeles, CA 90095-1562; shuping@astro.ucla.edu

JOHN BALLY

Center for Astrophysics and Space Astronomy, University of Colorado at Boulder,
Campus Box 389, Boulder, CO 80309-0389; bally@casa.colorado.edu

MARK MORRIS

Division of Astronomy and Astrophysics, University of California at Los Angeles,
Los Angeles, CA 90095-1562; morris@astro.ucla.edu

AND

HENRY THROOP

Department of Space Studies, Southwest Research Institute,
1050 Walnut Street, Suite 400, Boulder, CO 80302

ABSTRACT

We present a Brα ($\lambda = 4.05$ μm) image of the largest silhouette proplyd in Orion (114-426) using the facility near-IR spectrometer NIRSPEC at the Keck Observatory. This is the longest wavelength observation of a silhouette disk to date. The diameter of the disk at 4 μm is only marginally smaller than that observed in the optical with the *Hubble Space Telescope*. This may be the first signature of chromatic extinction for the translucent outer edges of the disk, suggesting that the near-IR opacity is dominated by processed grains with typical sizes greater than 1.9 μm, but *not* $\gg$4 μm.

Subject headings: circumstellar matter — dust, extinction — stars: formation — stars: pre–main-sequence

1. INTRODUCTION

Planets are thought to form out of the dust and gas orbiting young stellar objects. For planets to form, dust grains in these disks must grow beyond typical grain sizes found in the interstellar medium (ISM). Searches for evidence of grain growth, however, have produced mixed results. The dust in disks around young stellar objects and main-sequence stars has been primarily detected and studied using far-infrared through centimeter-wavelength continuum emission. However, spatially resolved images of disks either from continuum emission or scattered light are extraordinarily important since they can be used to constrain models of disk structure and to infer the existence of planets (Koerner, Sargent, & Ostroff 2001; Weinberger et al. 2002). Images of disks in extinction against a constant intensity background (i.e., in silhouette) can, in principle, also be used to constrain disk models, although these sources are very rare. In this Letter, we present new observations at ∼4 μm of one of the silhouette disks seen against the Orion Nebula.

The *Hubble Space Telescope* (*HST*) has produced dramatic images of protoplanetary disks ("proplyds") surrounding young stars in the Orion Nebula (O'Dell, Wen, & Hu 1993; McCaughrean & O'Dell 1996; O'Dell & Wong 1996; Bally et al. 1998; Bally, O'Dell, & McCaughrean 2000). The intense ultraviolet (UV) radiation field of the high-mass Trapezium stars heats the disk surfaces, drives mass loss, and produces bright ionization fronts (Johnstone et al. 1998). Proplyds are thought to contain young ($<10^6$ yr old) low-mass stars that are part of the Orion Nebula cluster (Hillenbrand 1997). The photoeva-

poration of these disks places strong temporal constraints on planet formation mechanisms in irradiated environments, which is important since a significant fraction of stars form in clusters with high-mass stars (Blaauw 1991).

Protostellar disks in Orion can be seen in silhouette against the nebular background or against the proplyd's own ionization front. To provide the highest contrast, silhouette disks are best observed using narrowband filters centered on a bright nebular emission line. The proplyd 114-426 is the largest of these silhouette disks, with a diameter of ∼2″, or ∼1000 AU at the distance of the Orion Nebula.[2] The grain properties in these disks can be studied via the wavelength dependence of attenuation of background light through the translucent disk edges. For grain sizes much smaller than the wavelengths observed (Rayleigh scattering limit), shorter wavelength radiation will be scattered much more efficiently than at longer wavelengths, causing the disk to appear "smaller" at long wavelengths. For grain sizes much larger than the wavelengths observed, the opacity will change little as a function of wavelength ("gray" scattering), rendering the disk size unchanged.

Here we present new observations of the 114-426 disk in silhouette against the nebular Brα emission at 4.05 μm using the facility near-IR spectrometer NIRSPEC (McLean et al. 1998) on the Keck II telescope. Previous *HST* observations in Hα and Pα suggest that the grains in the disk have grown to sizes larger than a few microns (Throop et al. 2001). A comparison of our Brα image with the previous *HST* images shows that the outer translucent edges of the disk are becoming more transparent, suggesting that the grain size distribution is not dominated by particles much larger than 4 μm.

---

[2] Throughout this Letter, we will adopt $d = 460$ pc for the distance to the Orion Nebula. Distance estimates to the Orion region range between 400 and 500 pc in the literature. See footnote 4 of Bally et al. (2000) for discussion and additional references.
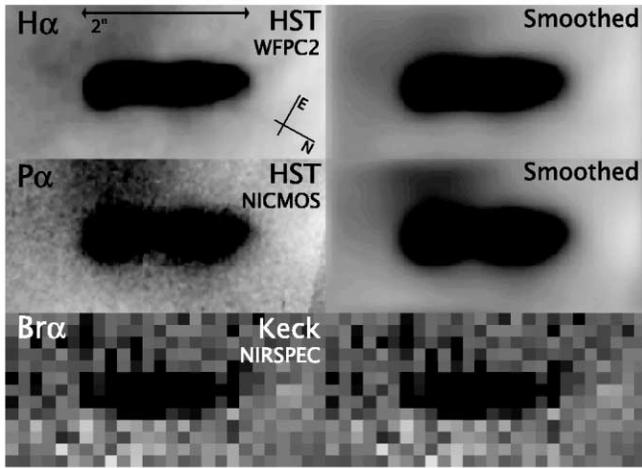
Fig. 1.—Observations of the 114-426 disk at Hα (0.656 μm; *HST*/WFPC2), Pα (1.87 μm; *HST*/NICMOS1), and Brα (4.05 μm; Keck/NIRSPEC) displayed on the same spatial scale. In the left panels, each image is shown at native resolution: FWHM(Hα) = 69 mas, FWHM(Pα) = 196 mas, and FWHM(Brα) = 360 mas. In the right panels, the *HST* images are shown smoothed to the resolution of the Keck Brα image (the left and right Keck Brα images are identical). The spatial scale for the Brα image is 198 mas pixel^{-1} along the long axis of the disk and 180 mas pixel^{-1} along the minor axis; see text for discussion.

Fig. 2.—Normalized intensity cuts along the major axis of the disk at matched resolution at Hα, Pα, and Brα. For the Hα and Pα data, the cut has been made after the image was smoothed to the Brα resolution (FWHM = 360 mas). The Keck Brα intensity cut has been smoothed with a 3 pixel running boxcar and is shown with 1 σ uncertainties. The hump at the center of the Pα disk is due to beam smearing of light from the pinched waist of the disk.

2. OBSERVATIONS AND ANALYSIS

The proplyd 114-426 was observed with NIRSPEC (McLean et al. 1998) on Keck II on UT 2002 January 2. All observations were made in high-resolution (cross-dispersed) mode with the 0″.144 × 12″ slit. The scale in the spectral direction was 4.3 km s^{-1} pixel^{-1}, and the resolution was measured to be 6.6 km s^{-1} ($R = 45,400$) using calibration lamp lines. The spatial scale along the slit is 198 mas pixel^{-1}. A data cube from 3.3 to 4.08 μm was made by aligning the slit with the long axis of the 114-426 disk (position angle = 29°) and stepping the slit in 180 mas (1 pixel in the NIRSPEC slit viewing camera, SCAM) increments perpendicular to the slit. Using observations of a standard star in low-resolution mode, we measured the seeing at 4 μm to be FWHM ≈ 360 mas. Thus, in the images extracted from the data cube, the scale along the slit direction (disk major axis) is 198 mas pixel^{-1} while the scale perpendicular to the slit (disk minor axis) is 180 mas pixel^{-1}.

The accuracy of telescope offsets perpendicular to the slit was determined by examination of *K*-band SCAM images of stars. Offset pointing accuracy was determined to be better than 1 180 mas SCAM pixel.

For each slit position, we summed over the wavelengths containing the Brα nebular emission line (4.05 μm) to produce a one-dimensional slit image. The high dispersion allowed us to perform a thermal background subtraction using spectral regions in between the telluric airglow lines. Thirteen slit positions were stacked to form a single two-dimensional image. A significant "striping" pattern on the chip was removed by building a flat field directly from the data cube and dividing into the background-subtracted image. The final image is shown in Figure 1; the effective "bandpass" is 21.5 km s^{-1} (5 pixels) centered on Brα (4.05 μm). The signal-to-noise ratio (S/N) in the continuum is 14. Since we are concerned primarily with the transmitted background nebular emission, flux calibration (which is quite difficult at ∼4 μm) is not necessary for our analysis.

To examine the disk structure and grain properties, we com-

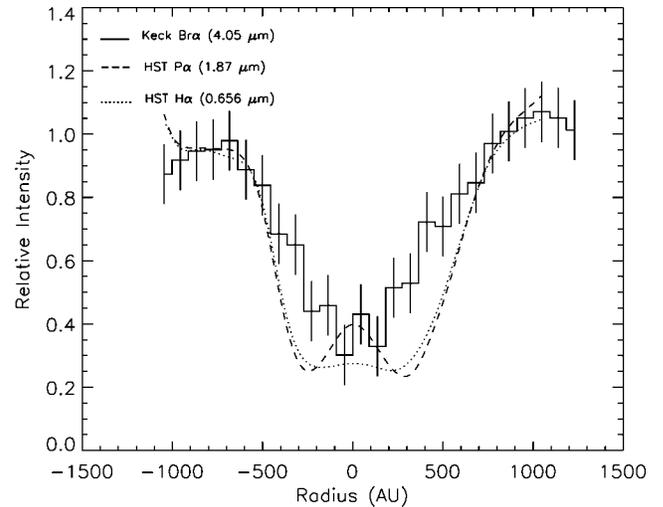pare the Brα image of the 114-426 disk to *HST* images in Hα (0.656 μm) and Pα (1.87 μm) (Fig. 1). A set of four dithered 400 s Hα images were obtained with the Wide Field Planetary Camera 2 (WFPC2; F656N) on 1999 January 11 as part of a larger narrowband survey of the Orion Nebula (Bally et al. 2000). The final reduced image has an angular resolution of FWHM(Hα) = 69 mas (30 AU). A single 640 s Pα image was obtained with NICMOS1 (F187N) on 1998 February 26 (Throop et al. 2001) with a resolution of FWHM(Pα) = 196 mas (69 AU).

In order to accurately compare the three narrowband images, we matched resolutions by convolving the *HST* narrowband images with the appropriate Gaussian so that the resulting, smoothed image has the same resolution as the Keck Brα data (FWHM = 360 mas). This smoothing softens the disk edges and also smears light from the disk edges into the central opaque regions of the silhouette. We then extracted intensity slices along the major axis of the disk for all three filters. The intensity was averaged over one FWHM of a seeing element (360 mas) perpendicular to the major axis. The background nebular intensity varies significantly across the *HST* images, with a strong gradient from south to north. We estimated the background intensity across the disk by averaging intensity cuts above and below the disk and smoothing the result. This synthetic nebular background was then used to normalize the disk intensity cuts. In addition, the Keck Brα intensity was smoothed with a 3 pixel running boxcar. Figure 2 shows the resulting intensity cuts along the major axis of the disk in all three filters. The "hump" at the center of the Pα disk is due to beam smearing of light from the pinched "waist" of the disk. In Hα and Pα, the diameter of the disk along the major axis is FWHM = 2″.22 ± 0″.04 and 2″.26 ± 0″.06 (1020 ± 20 and 1040 ± 30 AU), respectively. The errors in diameter for the *HST* data are due to uncertainties in the background normalization and represent the probable range of values for the FWHM. At Brα, the diameter is FWHM = 1″.9 ± 0″.2 (860 ± 90 AU): ∼80% of the width at Hα and Pα. For Brα, the error is dominated by the noise in the data itself (S/N = 14). The thickness of the disk along the minor axis in

Brα is less certain because the image is only marginally resolved perpendicular to the slit.

HST images of the proplyd 114-426 at Pα were first obtained with NICMOS1 on 1997 April 19. Based on these observations, McCaughrean et al. (1998) concluded that the 114-426 disk is ∼20% smaller in Pα than Hα. More recent analysis has shown, however, that the noise in the 1997 Pα data is too great to support this claim (Throop 2001). The 114-426 images from 1998 and 1999 are of much higher quality than those presented in McCaughrean et al. (1998) and clearly show that the disk is nearly the same width at Hα and Pα (Throop et al. 2001).

The lack of significant size difference between the more recent Hα and Pα *HST* images clearly indicates gray extinction for $\lambda \lesssim 1.9$ μm in the outer translucent portions of the 114-426 disk (Throop et al. 2001). The slight decrease in disk size at Brα, however, indicates that the outer edges of the disk are becoming more transparent at 4 μm. Hence, the size of typical scatterers in the outer portion of the 114-426 disk must be $\gtrsim 1.9$ μm but cannot be $\gg 4$ μm. In Figure 3, we plot some standard extinction curves for "typical" grains found in the ISM (Cardelli, Clayton, & Mathis 1989). Overplotted are values of A_V measured at the translucent northeast ansa of the disk (projected radius ∼400 AU), which suggests that the near-IR opacity in this region is dominated by processed grains that are significantly larger than those found in the ISM. No conclusions can be drawn regarding the opaque central regions of the disk.

3. DISCUSSION

One of us has developed a numerical model of grain evolution in protostellar disks subject to photoevaporation, which shows that grains grow most rapidly in the center of the disk where the highest temperatures and densities are found (Throop et al. 2001; Throop 2001). The growth rate decreases with distance from the central star; grain sizes reach 1 m at 10 AU and 1 mm at 500 AU in 10^5 yr, which is less than the median age of the Orion Nebula cluster (3×10^5 yr; Hillenbrand 1997). Although the age of 114-426 is unknown, the analysis presented here for the 114-426 disk is consistent with these grain growth models.

Protostellar disks near a strong source of UV radiation (e.g., a small cluster of O stars) are subject to photoevaporation, which radically alters the disk on relatively short timescales. Soft UV photons heat the disk surface layers ($N_H \sim 10^{21}$ cm^{-2}) to 1000 K and drive a photoablation flow, which then produces cometary ionization fronts (created by the far-UV flux) and standoff bow shocks with the O star wind (Johnstone et al. 1998; Bally et al. 1998, 2000). Mass loss can be as high as $10^{-6} M_\odot$ yr^{-1} (Johnstone et al. 1998; Henney & O'Dell 1999). Circumstellar disks within 1 pc of the Trapezium stars in Orion can be completely evaporated within the lifetime of the cluster (10^5 yr, assuming $M_{disk} = 0.01$–0.05 $M_\odot$). Small grains are entrained in this neutral flow if the gas drag exceeds gravity. Since grain growth is occurring at the same time, however, the disk will not be completely destroyed. Grains in the outer edge of the disk (which do not grow very fast) are easily lost, while large grains built up in the center of the disk are retained. Grain growth models indicate that after 10^5 yr a disk can be eroded from $R = 500$ AU down to ∼40 AU, where an edge of centimeter-sized particles is left behind. The large size of the 114-426 disk (compared to other proplyd disks in Orion) suggests either that it has not been subject to a significant photoevaporating radiation field or that the gas has already been
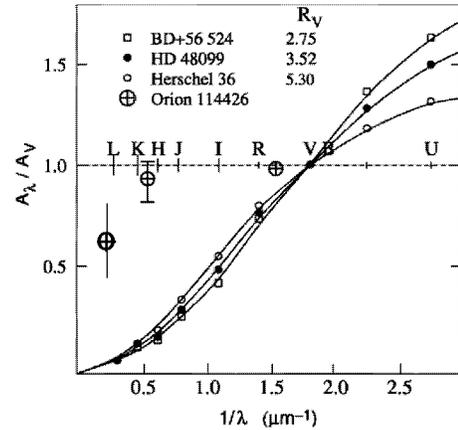
FIG. 3.—Extinction measurements (A_V) at the translucent northeast side of the disk compared to standard interstellar extinction curves (Cardelli et al. 1989).

removed and the disk consists of predominantly large particles and some smaller dust produced by grain-grain collisions (secondary production).

Although the growth of grains to large sizes is predicted in the previously discussed models, not all disks show evidence of large particles. Near-IR scattered light observations of the HR 4796A, HH 30, and GM Aurigae disks suggest typical grain sizes larger than that found in the ISM (Schneider et al. 1999, 2003; Cotera et al. 2001); and flat submillimeter spectra for several disks in Taurus and NGC 2024 point to the same conclusion (Mannings & Emerson 1994; Visser et al. 1998). However, NICMOS and WFPC2 scattered light images of other circumstellar disks in Taurus suggest grain parameters typical of the ISM (Burrows et al. 1996; Krist, Stapelfeldt, & Watson 2002; McCabe, Duchêne, & Ghez 2002). Submillimeter observations of HL Tau are inconclusive (Beckwith, Henning, & Nakagawa 2000). Each type of study, however, is most sensitive to dust in different spatial regions of the disk: the submillimeter flux is generated by thermal emission from grains in the midplane; scattered light is dominated by grains at the disk surface; and the observed size and structure of silhouette disks is governed by grains in the outer translucent edges. If the gas and dust are *not* well mixed (owing to settling, for example), then we should not expect these various techniques to produce the same results. In addition, there could certainly be differences in dust properties due to the star-forming environment, local history, and evolutionary state (e.g., older disks should have larger particles).

The initial phases of planet formation in protostellar disks are thought to require dust grain growth up to roughly centimeter-sized particles (Beckwith et al. 2000). The results presented here for 114-426 suggest that planet formation may be underway in this disk. Further observations at longer wavelengths, however, are required to assess grain growth in the central portions of the disk before any real conclusions regarding planet formation can be made.

We have presented here the longest wavelength image of a protostellar disk seen in silhouette using NIRSPEC on the Keck II telescope. The slightly reduced size of the disk at Brα compared to *HST* observations at Hα and Pα indicates the onset of chromatic extinction at about 4 μm. Extinction measurements in the outer translucent edges of the disk suggest that the opacity is dominated by grains that are significantly larger than those found in the ISM (but not $\gg 4$ μm). We plan to

undertake a more rigorous analysis of the dust grain population in the 114-426 disk by simultaneously modeling the narrow-band extinction images and the broadband images of the bipolar reflection nebulae also observed in this object. In addition, we plan mid-IR observations in an effort to determine the thermal properties of the grains in the midplane. These complementary observations and analyses should enable us to put much stricter limits on the grain properties for the 114-426 protostellar disk than those that have been derived for other protostellar systems.

REFERENCES

Bally, J., O'Dell, C. R., & McCaughrean, M. J. 2000, AJ, 119, 2919
Bally, J., Sutherland, R. S., Devine, D., & Johnstone, D. 1998, AJ, 116, 293
Beckwith, S. V. W., Henning, T., & Nakagawa, Y. 2000, in Protostars and Planets IV, ed. V. Manning, A. P. Boss, & S. S. Russell (Tucson: Univ. Arizona Press), 533
Blaauw, A. 1991, in The Physics of Star Formation and Early Stellar Evolution, ed. C. J. Lada & N. D. Kylafis (NATO ASIC Ser. C, 342; Dordrecht: Kluwer), 125
Burrows, C. J., et al. 1996, ApJ, 473, 437
Cardelli, J. A., Clayton, G. C., & Mathis, J. S. 1989, ApJ, 345, 245
Cotera, A. S., et al. 2001, ApJ, 556, 958
Henney, W. J., & O'Dell, C. R. 1999, AJ, 118, 2350
Hillenbrand, L. A. 1997, AJ, 113, 1733
Johnstone, D., Hollenbach, D., & Bally, J. 1998, ApJ, 499, 758
Koerner, D. W., Sargent, A. I., & Ostroff, N. A. 2001, ApJ, 560, L181
Krist, J. E., Stapelfeldt, K. R., & Watson, A. M. 2002, ApJ, 570, 785

Mannings, V., & Emerson, J. P. 1994, MNRAS, 267, 361
McCabe, C., Duchêne, G., & Ghez, A. M. 2002, ApJ, 575, 974
McCaughrean, M. J., & O'Dell, C. R. 1996, AJ, 111, 1977
McCaughrean, M. J., et al. 1998, ApJ, 492, L157
McLean, I. S., et al. 1998, Proc. SPIE, 3354, 566
O'Dell, C. R., Wen, Z., & Hu, X. 1993, ApJ, 410, 696
O'Dell, C. R., & Wong, K. 1996, AJ, 111, 846
Schneider, G., Wood, K., Silverstone, M., Hines, D. C., Koerner, D. W., Whitney, B. A., Bjorkman, J. E., & Lowrance, P. J. 2003, AJ, 125, 1467
Schneider, G., et al. 1999, ApJ, 513, L127
Throop, H. B. 2001, Ph.D. thesis, Univ. Colorado, Boulder
Throop, H. B., Bally, J., Esposito, L. W., & McCaughrean, M. J. 2001, Science, 292, 1686
Visser, A. E., Richer, J. S., Chandler, C. J., & Padman, R. 1998, MNRAS, 301, 585
Weinberger, A. J., et al. 2002, ApJ, 566, 409